J|A|C|S
ARTICLES
Published on Web 11/14/2006

Helical Metallohost−Guest Complexes via Site-Selective Transmetalation of Homotrinuclear Complexes

Shigehisa Akine, Takanori Taniguchi, and Tatsuya Nabeshima*

Contribution from the Department of Chemistry, University of Tsukuba, Tsukuba, Ibaraki 305-8571, Japan

Received July 12, 2006; E-mail: nabesima@chem.tsukuba.ac.jp

Abstract: We have designed a new type of bis(N_2O_2) chelate ligand that affords a C-shaped O_6 site on the metalation of the N_2O_2 sites. UV−vis and ^{1}H NMR titration clearly showed that the complexation between H_4L and zinc(II) acetate affords 1:3 complex $[LZn_3]^{2+}$ via a highly cooperative process. Although the O_6-recognition site of the dinuclear metallohost $[LZn_2]$ is filled with the additional Zn^{2+}, the O_6 site can bind a guest ion with concomitant release of the initially bound Zn^{2+}. The novel recognition process "guest exchange" took place quantitatively when rare earth metals were used as a guest. In the case of alkaline earth metals, selectivity of $Ca^{2+} > Sr^{2+} > Ba^{2+} \gg Mg^{2+}$ was observed. On the other hand, the transmetalation did not take place at all when alkali metals were used for the guest. Accordingly, the trinuclear complex $[LZn_3]^{2+}$ is excellent in discriminating charge of the guest ions. The metallohost−guest complexes thus obtained have a helical structure, and the radius *d* and winding angle θ of the helix depend on the size of the guest. The La^{3+} complex has the smallest θ (288°), and the Sc^{3+} complex has the largest θ (345°). Because the radius and winding angles of helices are tunable by changing the guest ion, the helical metallohost−guest complexes are regarded as a molecular spring or coil. Consequently, site-specific metal exchange of trinuclear complex $[LZn_3]^{2+}$ described here will be utilized for highly selective ion recognition, site-selective synthesis of $(3d)_2(4f)$ trimetallic complexes, and construction of "tunable" metallohelicenes.

Introduction

Recently, metallohosts have attracted much interest because they would have various functions of the parent metal complexes. Photochemical[1] and redox[2] properties arising from hybridization between the organic and metal complex moieties are successfully applied to guest sensing or detection. Reversibility of coordination bonds between a metal and ligands is also an important factor to construct supramolecular metallohosts.[3] In particular, conversion of an acyclic molecule to the corresponding cyclic metallohost is effective to control guest recognition (Scheme 1A).[3] We have investigated allosteric regulation of guest recognition by pseudomacrocycles obtained by the complexation of bis- or tris(bipyridine) ligands with transition metals.[4] The unique strategy is also applied to sophisticated functions such as transduction of molecular information.[5]

Scheme 1. Two Strategies for Controllable Guest Binding System Utilizing Metal Coordination

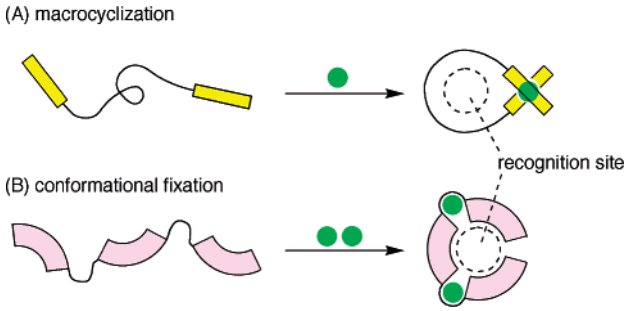

Salen-type N_2O_2 chelates are also attractive candidates for a metal-binding site to be incorporated into metallohosts.[6] Salen ligands coordinate to various kinds of transition and typical metals in a tetradentate fashion to give stable complexes, some of which are used as catalysts for organic reactions,[7] models of reaction centers of metalloenzymes,[8] nonlinear optical materials,[9]

(1) For reviews, see: (a) Fabbrizzi, L.; Licchelli, M.; Rabaioli, G.; Taglietti, A. *Coord. Chem. Rev.* **2000**, *205*, 85−108. (b) Robertson, A.; Shinkai, S. *Coord. Chem. Rev.* **2000**, *205*, 157−199. (c) Keefe, M. H.; Benkstein, K. D.; Hupp, J. T. *Coord. Chem. Rev.* **2000**, *205*, 201−228. (d) Rogers, C. W.; Wolf, M. O. *Coord. Chem. Rev.* **2002**, *233*−*234*, 341−350.

(2) For reviews, see: (a) Beer, P. D. *Chem. Commun.* **1996**, 689−696. (b) Beer, P. D. *Acc. Chem. Res.* **1998**, *31*, 71−80. (c) Beer, P. D.; Cadman, J. *Coord. Chem. Rev.* **2000**, *205*, 131−155. (d) Beer, P. D.; Hayes, E. J. *Coord. Chem. Rev.* **2003**, *240*, 167−189.

(3) (a) Nabeshima, T. *Coord. Chem. Rev.* **1996**, *148*, 151−169. (b) Nabeshima, T.; Akine, S.; Saiki, T. *Rev. Heteroat. Chem.* **2000**, *22*, 219−239.

(4) (a) Nabeshima, T.; Inaba, T.; Furukawa, N. *Tetrahedron Lett.* **1987**, *28*, 6211−6214. (b) Nabeshima, T.; Inaba, T.; Sagae, T.; Furukawa, N. *Tetrahedron Lett.* **1990**, *31*, 3919−3922. (c) Nabeshima, T.; Inaba, T.; Furukawa, N.; Hosoya, T.; Yano, Y. *Inorg. Chem.* **1993**, *32*, 1407−1416. (d) Nabeshima, T.; Yosejima, I.; Yano, Y. *Heterocycles* **1994**, *38*, 1471−1474. (e) Nabeshima, T.; Hosoya, T.; Yano, Y. *Synlett* **1998**, 265−266. (f) Nabeshima, T.; Hashiguchi, A.; Yazawa, S.; Haruyama, T.; Yano, Y. *J. Org. Chem.* **1998**, *63*, 2788−2789. (g) Nabeshima, T.; Hashiguchi, A. *Tetrahedron Lett.* **2002**, *43*, 1457−1459. (h) Nabeshima, T.; Yoshihira, Y.; Saiki, T.; Akine, S.; Horn, E. *J. Am. Chem. Soc.* **2003**, *125*, 28−29. (i) Nabeshima, T.; Saiki, T.; Iwabuchi, J.; Akine, S. *J. Am. Chem. Soc.* **2005**, *127*, 5507−5511. (j) Nabeshima, T.; Tanaka, Y.; Saiki, T.; Akine, S.; Ikeda, C.; Sato, S. *Tetrahedron Lett.* **2006**, *47*, 3541−3544.

(5) Nabeshima, T.; Hashiguchi, A.; Saiki, T.; Akine, S. *Angew. Chem., Int. Ed.* **2002**, *41*, 481−484.

(6) For reviews, see: (a) van Veggel, F. C. J. M.; Verboom, W.; Reinhoudt, D. N. *Chem. Rev.* **1994**, *94*, 279−99. (b) Verboom, W.; Rudkevich, D. M.; Reinhoudt, D. N. *Pure Appl. Chem.* **1994**, *66*, 679−86. (c) Antonisse, M. M. G.; Reinhoudt, D. N. *Chem. Commun.* **1998**, 443−448.

Scheme 2. Principle of Ion Recognition Based on Metal Exchange

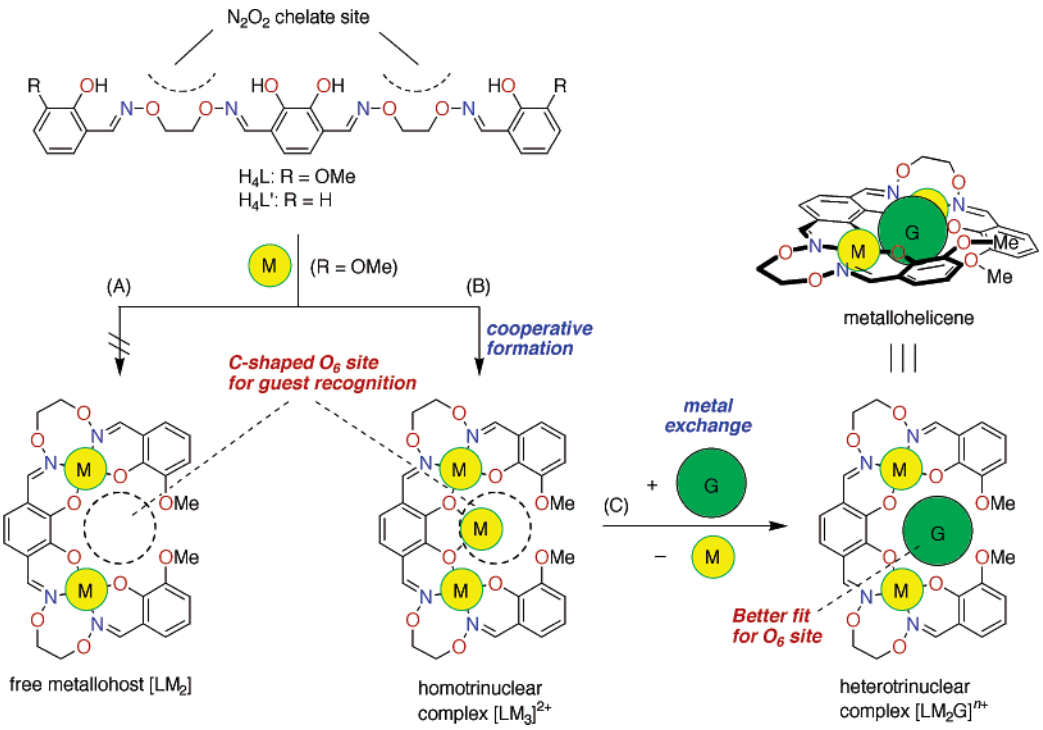

and building blocks for interlocked molecules.[10] To use salen moieties to control guest recognition, a strategy different from the macrocyclization seems to be also useful because a salen−metal complex constitutes one salen ligand and a metal. For example, conformational fixation of salen-type ligands by making four coordination bonds between the ligand and the metal ion (Scheme 1B) would work very efficiently. Thus, we designed a novel bis(N_2O_2) ligand H_4L to control guest binding by utilizing the coordination-triggered conformational changes (Scheme 2A). When the two salamo[11] moieties of H_4L are metalated, six oxygen atoms are fixed in an acyclic, C-shaped arrangement. The resultant 18-crown-6-like recognition site[12] would be suitable for ion recognition. In addition, the guest binding may be more favorable because the negatively charged phenolates of the complexes have a higher coordination ability to another metal (alkali,[13] alkaline earth,[14] rare earth,[15] etc.) than do their phenol form. Here, we report cooperative formation of trinuclear complex, instead of dinuclear complex, by the metalation of bis(salamo) ligand H_4L (Scheme 2B).[16] Although the O_6-recognition site was occupied by the third metal M, it can bind more strongly to metal ions having an appropriate size, replacing the M bound initially (Scheme 2C). The resultant metallohost−guest complexes $[LM_2G]^{n+}$ would have a helical conformation,[17] where the $[LM_2]$ metallohost moiety wraps the guest ion G^{n+}. Furthermore, the helical complexes are regarded as a tunable molecular spring or coil, because the radius and winding angle of the helical complexes depend on the guest ion G^{n+}.

Results and Discussion

Synthesis of the Ligands. A synthetic route to the new ligands H_4L and H_4L' is shown in Scheme 3. Dilithiation[18] of 1,2-dimethoxybenzene by *n*-butyllithium in the presence of TMEDA followed by the addition of DMF afforded 2,3-dimethoxybenzene-1,4-dicarbaldehyde (**1**) in 40% yield. Demethylation of **1** with boron tribromide in dichloromethane gave 2,3-dihydroxybenzene-1,4-dicarbaldehyde (**2**)[19] in almost quan-

(7) For reviews, see: (a) Jacobsen, E. N. In *Catalytic Asymmetric Synthesis*; Ojima, I., Ed.; VCH: New York, 1993. (b) Katsuki, T. *Coord. Chem. Rev.* **1995**, *140*, 189−214. (c) Jacobsen, E. N. *Acc. Chem. Res.* **2000**, *33*, 421−431.
(8) (a) Tsou, T.-T.; Loots, M.; Halpern, J. *J. Am. Chem. Soc.* **1982**, *104*, 623−624. (b) Summers, M. F.; Marzilli, L. G.; Bresciani-Pahor, N.; Randaccio, L. *J. Am. Chem. Soc.* **1984**, *106*, 4478−4485.
(9) (a) Di Bella, S.; Fragalà, I. *Synth. Met.* **2000**, *115*, 191−196. (b) Lacroix, P. G. *Eur. J. Inorg. Chem.* **2001**, 339−348.
(10) Yoon, I.; Narita, M.; Shimizu, T.; Asakawa, M. *J. Am. Chem. Soc.* **2004**, *126*, 16740−16741.
(11) H_2salamo = 1,2-bis(salicylideneaminooxy)ethane, see: (a) Akine, S.; Taniguchi, T.; Nabeshima, T. *Chem. Lett.* **2001**, 682−683. (b) Akine, S.; Taniguchi, T.; Nabeshima, T. *Inorg. Chem.* **2004**, *43*, 6142−6144. (c) Akine, S.; Taniguchi, T.; Dong, W.; Masubuchi, S.; Nabeshima, T. *J. Org. Chem.* **2005**, *70*, 1704−1711. (d) Akine, S.; Nabeshima, T. *Inorg. Chem.* **2005**, *44*, 1205−1207. (e) Akine, S.; Dong, W.; Nabeshima, T. *Inorg. Chem.* **2006**, *45*, 4677−4684.
(12) For reviews on self-assembled metallacrown ethers, see: (a) Pecoraro, V. L.; Stemmler, A. J.; Gibney, B. R.; Bodwin, J. J.; Wang, H.; Kampf, J. W.; Barwinski, A. In *Progress in Inorganic Chemistry 45*; Karlin, K. D., Ed.; Wiley: New York, 1996; Chapter 2, pp 83−177. (b) Bodwin, J. J.; Cutland, A. D.; Malkani, R. G.; Pecoraro, V. L. *Coord. Chem. Rev.* **2001**, *216−217*, 489−512.
(13) (a) Armstrong, L. G.; Lip, H. C.; Lindoy, L. F.; McPartlin, M.; Tasker, P. A. *J. Chem. Soc., Dalton Trans.* **1977**, 1771−1774. (b) Giacomelli, A.; Rotunno, T.; Senatore, L. *Inorg. Chem.* **1985**, *24*, 1303−1306. (c) Giacomelli, A.; Rotunno, T.; Senatore, L.; Settambolo, R. *Inorg. Chem.* **1989**, *28*, 3552−3555. (d) Cunningham, D.; McArdle, P.; Mitchell, M.; Ní Chonchubhair, N.; O'Gara, M.; Franceschi, F.; Floriani, C. *Inorg. Chem.* **2000**, *39*, 1639−1649.
(14) Carbonaro, L.; Isola, M.; La Pegna, P.; Senatore, L.; Marchetti, F. *Inorg. Chem.* **1999**, *38*, 5519−5525.
(15) (a) Condorelli, G.; Fragalà, I.; Giuffrida, S.; Cassol, A. *Z. Anorg. Allg. Chem.* **1975**, *412*, 251−257. (b) Costisor, O.; Linert, W. *Rev. Inorg. Chem.* **2005**, *25*, 13−54.
(16) (a) Akine, S.; Taniguchi, T.; Nabeshima, T. *Angew. Chem., Int. Ed.* **2002**, *41*, 4670−4673. (b) Akine, S.; Taniguchi, T.; Saiki, T.; Nabeshima, T. *J. Am. Chem. Soc.* **2005**, *127*, 540−541. (c) Akine, S.; Matsumoto, T.; Taniguchi, T.; Nabeshima, T. *Inorg. Chem.* **2005**, *44*, 3270−3274.
(17) For reviews on helical metalloarchitectures, see: (a) Constable, E. C. *Tetrahedron* **1992**, *48*, 10013−10059. (b) Lehn, J.-M. *Supramolecular Chemistry, Concepts and Perspectives*; VCH: Weinheim, 1995. (c) Piguet, C.; Bernardinelli, G.; Hopfgartner, G. *Chem. Rev.* **1997**, *97*, 2005−2062.
(18) Crowther, G. P.; Sundberg, R. J.; Sarpeshkar, A. M. *J. Org. Chem.* **1984**, *49*, 4657−4663.

Scheme 3. Synthesis of Bis(N_2O_2-chelate) Ligands H_4L and H_4L'[a]

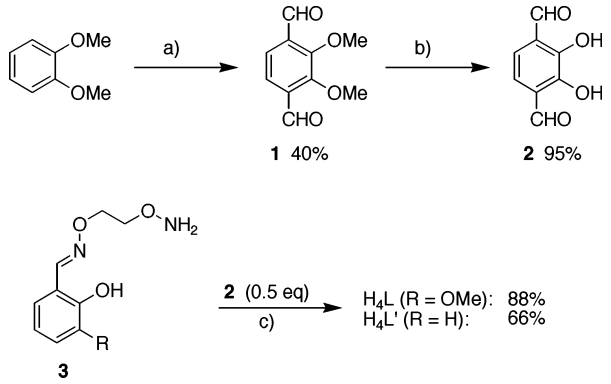

[a] Reagents and conditions: (a) (i) *n*-BuLi, TMEDA, Et_2O, (ii) DMF then H_2O; (b) BBr_3, CH_2Cl_2 then H_2O; (c) EtOH.

titative yield. The reaction of monooximes **3** (R = OMe, H)[11c] with dialdehyde **2** in ethanol gave the bis(salamo) ligands H_4L and H_4L' in 88% and 66% yield, respectively.

Metalation of Bis(N_2O_2) Ligands with d-Block Metals. The metalation of two N_2O_2 sites of the bis(salamo) ligand H_4L with zinc(II) was investigated by spectroscopic methods. Although H_4L has two salamo-chelate moieties, ^{1}H NMR titration (Figure 1) clearly indicates formation of a 1:3 complex,[20] which was also ascertained by an intense peak at m/z = 829.0 $[LZn_3(OAc)]^+$ in the ESI mass spectrum. The ^{1}H NMR spectra of H_4L in the presence of 1−2 equiv of zinc(II) acetate exhibit only two sets of signals, which can be assigned to free ligand H_4L and the zinc(II) complex. Because no other complexes with a different stoichiometry such as 1:1 and 1:2 were observed in the spectra, the complexation took place in a highly cooperative fashion. The cooperative triple metalation was also confirmed by the isosbestic points in the absorption spectra.

From a 1:3 mixture of ligand H_4L and zinc(II) acetate, a yellow crystalline complex of $[LZn_3(OAc)_2(H_2O)]$ was isolated. X-ray crystallography revealed that the complex contains one ligand L, three zinc atoms, two acetato ligands, and one water molecule (Figure 2A). Two of the three zinc atoms (Zn1 and Zn3) sit in the N_2O_2 salamo moieties, while Zn2 is located in the central O_6 site. Two oxygen atoms (O5 and O6) of the O_6 site bridge Zn1−Zn2 and Zn2−Zn3, respectively. In addition, two μ-acetato ligands linking Zn1 to Zn2 and Zn2 to Zn3 also stabilize the trinuclear structure. The central zinc atom, Zn2, has an aqua ligand. Thus, two of the three zinc atoms, Zn1 and Zn3, have a pentacoordinate trigonal bipyramidal geometry, in which the axial positions are occupied by N1−O5 and N4−O6, respectively. On the other hand, Zn2 has a square pyramidal geometry where the apical position is occupied by the aqua ligand (O15). We have already reported that all three zinc atoms of $[LZn_3(OAc)_2(EtOH)]$ have a trigonal bipyramidal geometry.[16a] Two hydrogen bonds (O15−O2 and O15−O9) probably change the geometry of Zn2 from trigonal bipyramidal to square pyramidal. Although the central metal (Zn2) sits in the O_6 cavity, four of the six oxygen atoms (O1, O2, O9, and O10) do not coordinate to Zn2. The ligand H_4L', which has no methoxy

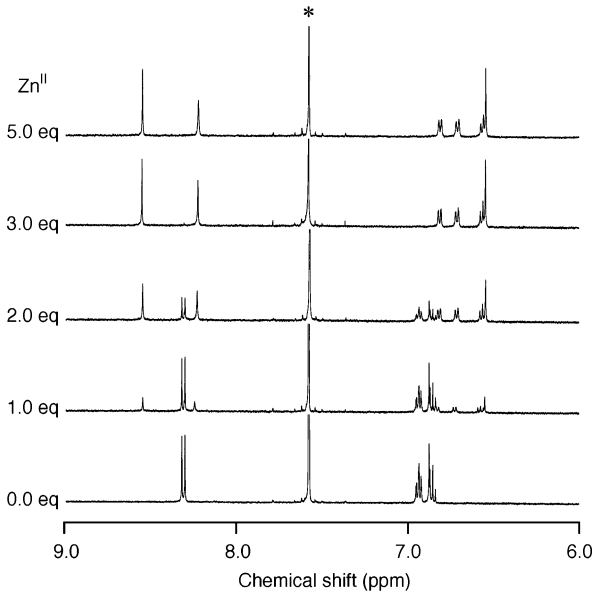

Figure 1. ^{1}H NMR spectral changes of H_4L by the addition of zinc(II) acetate (400 MHz, $CDCl_3/CD_3OD$ (1:1), $[H_4L]$ = 1.0 mM). Asterisk denotes solvent signal.

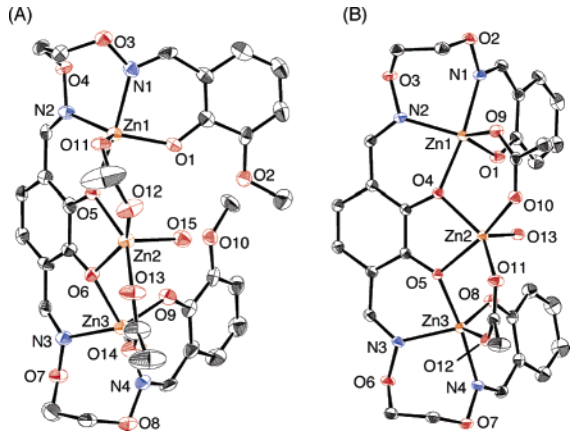

Figure 2. Crystal structures of (A) $[LZn_3(OAc)_2(H_2O)]$ and (B) $[L'Zn_3(OAc)_2(H_2O)]$. Thermal ellipsoids are drawn at 50% probability level. Hydrogen atoms and solvent molecules are omitted for clarity.

groups, also gave a similar trinuclear complex $[L'Zn_3(OAc)_2(H_2O)]$ (Figure 2B).

The stabilization by the acetato ligands may be closely related to the high cooperativity. If the complexation takes place at the N_2O_2 salamo sites (Scheme 4 , (i) and (ii)), intermediates (A) and (B) are formed. Yet only trinuclear complex $[LZn_3]^{2+}$ was observed, even if less than 3 equiv of zinc(II) acetate was added. This indicates that the complexation at the O_6 site (only two coordination bonds between ligand L^{4-} and Zn^{2+}) occurs immediately after the complexation at the N_2O_2 sites (four coordination bonds at each site). The trinuclear complex $[LZn_3]^{2+}$ is more stable than the possible intermediates (A−C), probably due to the increased number of bridging acetato ligands as well as μ-phenoxo moieties.

Transmetalation of $[LZn_3]^{2+}$ with Rare Earth Metals. Although the O_6-recognition site of the dinuclear metallohost $[LZn_2]$ is filled with the additional Zn^{2+}, the Zn^{2+} ion seems to be too small to fit. The O_6 site can bind a guest ion having an appropriate size with concomitant release of the initially bound Zn^{2+}. The ionic radius of lanthanides (1.30−1.12 Å for

(19) Akine, S.; Taniguchi, T.; Nabeshima, T. *Tetrahedron Lett.* **2001**, *42*, 8861−8864.
(20) Complexes having three metals in two different sites, see: (a) Albrecht, M.; Witt, K.; Röttele, H.; Fröhlich, R. *Chem. Commun.* **2001**, 1330−1331. (b) Fontecha, J. B.; Goetz, S.; McKee, V. *Angew. Chem., Int. Ed.* **2002**, *41*, 4553−4556. (c) Anderson, O. P.; la Cour, A.; Dodd, A.; Garrett, A. D.; Wicholas, M. *Inorg. Chem.* **2003**, *42*, 122−127.

Scheme 4. Proposed Mechanism for the Cooperative Formation of Trinuclear Complex $[LZn_3(OAc)_2(solv)]$

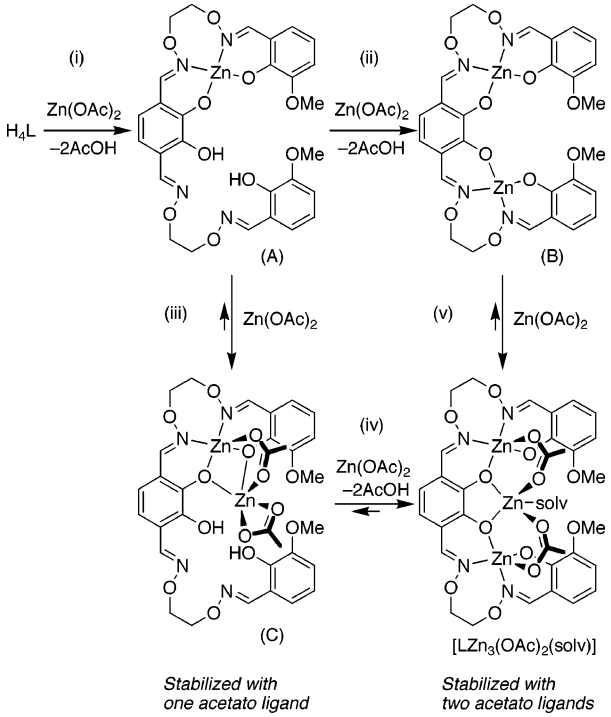

octacoordinate trivalent cations) is larger than that of zinc(II) (0.88 Å for hexacoordinate Zn^{2+}) and is suitable for the inclusion into the central O_6 site of the $[LZn_2]$ moiety. Thus, we expected that the trinuclear complex $[LZn_3]^{2+}$ would strongly bind to lanthanide(III) ions.

In the ESI mass spectrum of $[LZn_3]^{2+}$ in the presence of 1 equiv of Eu^{3+}, strong peaks at $m/z = 460.0$ $[LZn_2Eu(OAc)]^{2+}$ and 977.0 $[LZn_2Eu(OAc)_2]^{+}$ were observed. This strongly indicates the formation of a heterotrinuclear complex, $[LZn_2Eu]^{3+}$, via metal exchange.[21] No peaks attributed to 1:1 adduct $[LZn_3Eu]^{5+}$ or starting homotrinuclear $[LZn_3]^{2+}$ were observed. The metal exchange process was also investigated by the absorption spectrum. Upon treatment of a solution of $[LZn_3]^{2+}$ with $Eu(NO_3)_3$, the absorption band at 438 nm of $[LZn_3]^{2+}$ decreased. Concomitantly, a new absorption band at 370 nm due to the formation of a new species increased with isosbestic points at 426 and 364 nm (Figure 3). The spectral changes are completed by the addition of just 1 equiv of Eu^{3+}, implying that the metal exchange occurs in a 1:1 stoichiometry; that is, one Eu^{3+} replaces one Zn^{2+}.

The same complex $[LZn_2Eu(OAc)_2]^{+}$ was also formed when Zn^{2+} and Eu^{3+} were added to H_4L in the reverse order. Although no spectral changes were observed when 1 equiv of $Eu(NO_3)_3$ was added to a solution of H_4L, the addition of $Zn(OAc)_2$ to an equimolar mixture of H_4L and Eu^{3+} caused significant spectral changes. We obtained the spectrum identical to that of $[LZn_2Eu(OAc)_2]^{+}$ (Scheme 5A and B) when 3 equiv of $Zn(OAc)_2$ was added. The fact indicates that the complexation/decomplexation processes are fast enough to give the most thermodynamically stable complex.

(21) Transmetalation of hetero- to homometallic or homo- to homometallic complexes is reported in the case of compartmental complexes, see: (a) Atkins, A. J.; Black, D.; Blake, A. J.; Marin-Becerra, A.; Parsons, S.; Ruiz-Ramirez, L.; Schröder, M. *Chem. Commun.* **1996**, 457−464. (b) Furutachi, H.; Fujinami, S.; Suzuki, M.; Okawa, H. *J. Chem. Soc., Dalton Trans.* **2000**, 2761−2769. (c) Yonemura, M.; Arimura, K.; Inoue, K.; Usuki, N.; Ohba, M.; Okawa, H. *Inorg. Chem.* **2002**, *41*, 582−589.

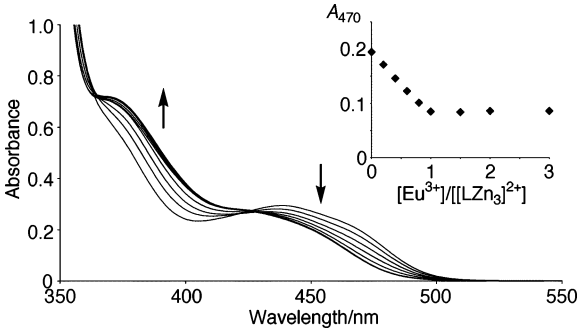

Figure 3. UV−vis spectral changes of $[LZn_3]^{2+}$ by the addition of $Eu(NO_3)_3$ in chloroform/methanol (1:1), $[H_4L] = 0.1$ mM, $[Zn(OAc)_2] = 0.3$ mM.

Scheme 5. Formation of $[LZn_2Eu(OAc)_2]^{+}$ by Three Methods

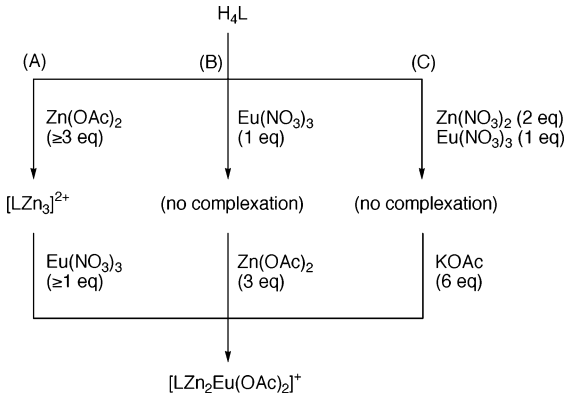

Thus, the titration experiment clearly showed 1:3:1 stoichiometry ($H_4L/Zn^{2+}/Eu^{3+}$), although the resultant complex $[LZn_2Eu]^{3+}$ has only two zinc ions. The result can be explained by the coordination of acetate ions to the trinuclear ZnEuZn core as follows. Formation of $[LZn_2Eu]^{3+}$ requires 2 equiv of $Zn(OAc)_2$, two Zn^{2+} for the N_2O_2 sites and four OAc^{-} for deprotonation of the phenol functionality. The heterotrinuclear complex $[LZn_2Eu]^{3+}$ may be stabilized by coordination of OAc^{-} on the basis of the observation of $[LZn_2Eu(OAc)_2]^{+}$ in the mass spectrum.

The importance of the coordination of OAc^{-} is also confirmed by the following experiment. A 1:3:1 mixture of H_4L, $Zn(NO_3)_2$, and $Eu(NO_3)_3$ showed an absorption spectrum identical to that of H_4L, indicating no complexation. Spectrophotometric titration of the mixture with KOAc showed that 6 equiv of KOAc was required to convert the mixture to $[LZn_2Eu(OAc)_2]^{+}$ (Scheme 5C). The 6 equiv of OAc^{-} consists of four for deprotonation and two for coordination to the trinuclear core.

It is noteworthy that a solution of H_4L containing excess $Zn(OAc)_2$ and $Eu(NO_3)_3$ (4 and 3 equiv, respectively) exhibited the spectrum identical to that of $[LZn_2Eu(OAc)_2]^{+}$. Thus, Zn^{2+} ions are bound selectively to the two salamo moieties and Eu^{3+} ion in the central cavity, even if there are excess amounts of Zn^{2+} and Eu^{3+} (Scheme 5A).

Spectrophotometric titration with other rare earth metals (G = La^{3+}−Lu^{3+}, Sc^{3+}, Y^{3+}) (Figures S1−S3) also exhibited 1:1 stoichiometry, indicating that the corresponding heterotrinuclear complexes $[LZn_2G]^{3+}$ were formed. In the case of smaller rare earth metals (G = Dy^{3+}, Ho^{3+}, Er^{3+}, Tm^{3+}, Yb^{3+}, Lu^{3+}, Y^{3+}, Sc^{3+}), the shoulder absorption at around 370 nm was weak.

The binding behavior of the metallohost $[LZn_3]^{2+}$ was investigated by ^1H NMR spectral changes in $CDCl_3/CD_3OD$

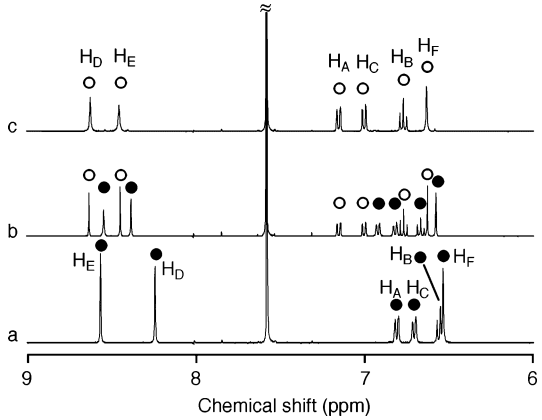

Figure 4. ^{1}H NMR spectra (400 MHz) of $[LZn_3]^{2+}$ in the presence of (a) 0, (b) 0.5, and (c) 1 equiv of $La(NO_3)_3$ in $CDCl_3/CD_3OD$ (1:1). The signals of $[LZn_2La]^{3+}$ and $[LZn_3]^{2+}$ are indicated with ○ and ●, respectively. Assignments of the signals are based on 2D-COSY and NOESY spectra; see Scheme 6 for atom labeling.

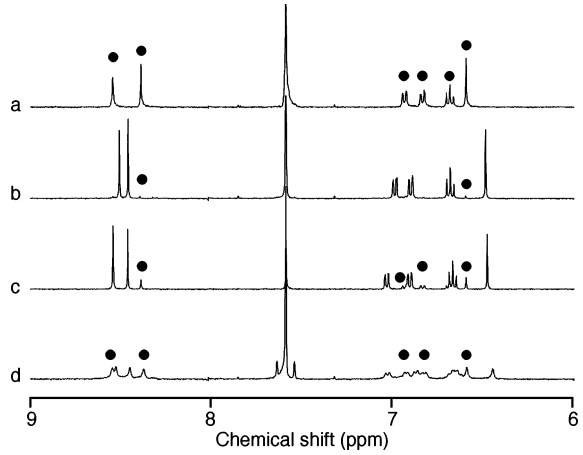

Figure 5. ^{1}H NMR spectra (400 MHz) of $[LZn_3]^{2+}$ in $CDCl_3/CD_3OD$ (1:1) in the presence of 2 equiv of $G(ClO_4)_2$. (a) G = Mg; (b) G = Ca; (c) G = Sr; (d) G = Ba. The signals of remaining $[LZn_3]^{2+}$ are indicated with ●.

(1:1) on the addition of diamagnetic $La(NO_3)_3$ (Figure 4). In the spectra, a new set of signals appeared separately from the initial homotrinuclear complex $[LZn_3]^{2+}$. The metallohost $[LZn_3]^{2+}$ was completely converted to $[LZn_2La]^{3+}$ when 1 equiv of La^{3+} was added. Because one zinc ion in $[LZn_3]^{2+}$ was liberated concomitantly with the complexation with La^{3+}, the complexation process is formulated as the guest-exchange equilibrium shown in Scheme 6. The equilibrium constant K_{La} is calculated to be >1000 on the basis of the remaining $[LZn_3]^{2+}$ less than the detection limit of ^{1}H NMR ($[LZn_3]^{2+}/[LZn_2La]^{3+}$ < 0.03). Similarly, $[LZn_3]^{2+}$ was quantitatively converted to $[LZn_2G]^{3+}$ when other rare earth ions (G = Sc^{3+}, Y^{3+}, Eu^{3+}, Lu^{3+}) were added. The equilibrium constants for these ions are very large (K_G > 1000).

We have already shown that ligand H_4L' without methoxy groups at the terminals gives homotrinuclear complex $[L'Zn_3]^{2+}$ similar to the methoxy analogue. However, transmetalation of $[L'Zn_3]^{2+}$ with La^{3+} was significantly disfavored. Addition of La^{3+} to $[L'Zn_3]^{2+}$ resulted in new sets of signals for several kinds of complexes, but a considerable amount of $[L'Zn_3]^{2+}$ remained even in the presence of 3 equiv of La^{3+}. Consequently, the methoxy groups of H_4L are indispensable for the efficient transmetalation. Six donor atoms including methoxy groups, having a C-shaped arrangement, effectively coordinate to rare earth guest G^{3+} (see X-ray structures). The stabilization by the resultant six coordination bonds probably shifts the guest-exchange equilibrium to give heterotrinuclear complex $[LZn_2G]^{3+}$.

Transmetalation of $[LZn_3]^{2+}$ with Alkali and Alkaline Earth Metals. In biological studies, lanthanides are frequently used to explore the Ca^{2+}-binding sites of proteins because the ionic radius of Ca^{2+} is similar to those of lanthanide(III) ions.[22] In the present case, $[LZn_3]^{2+}$ is also expected to bind Ca^{2+} strongly on the basis of the high lanthanide affinity. Thus, we investigated the binding affinity of $[LZn_3]^{2+}$ to alkali and alkaline earth metals.

When Ca^{2+} was added to the metallohost $[LZn_3]^{2+}$ in $CDCl_3/CD_3OD$ (1:1), a new set of signals, attributable to $[LZn_2Ca]^{2+}$, appeared in the ^{1}H NMR spectrum. When 2 equiv of Ca^{2+} was added, 97% of $[LZn_3]^{2+}$ was converted to the calcium complex (Figure 5b). The equilibrium constant (K_{Ca} = 32 ± 3) was calculated by nonlinear least-squares regression (Table 1). Formation of the heterotrinuclear complex was supported by the peak at m/z = 805.0 $[LZn_2Ca(OAc)]^+$ in the ESI mass spectrum, and the 1:1 ($Ca^{2+}/[LZn_3]^{2+}$) stoichiometry was confirmed by spectrophotometric titration (Figure S4).

Addition of Sr^{2+} to $[LZn_3]^{2+}$ resulted in similar ^{1}H NMR spectral changes, indicative of the formation of the corresponding heterotrinuclear complex $[LZn_2Sr]^{2+}$ (Figure 5c; K_{Sr} = 3.9 ± 0.6). On the contrary, transmetalation with Ba^{2+} took place less efficiently. About 50% of $[LZn_3]^{2+}$ remained even in the presence of 2 equiv of Ba^{2+} (Figure 5d). The equilibrium constant (K_{Ba} = 0.16 ± 0.04) was much smaller than those of Ca^{2+} and Sr^{2+}. It is noteworthy that the transmetalation did not take place when Mg^{2+} was added. Only the starting homotrinuclear complex $[LZn_3]^{2+}$ was detected in the ESI spectrum of an equimolar mixture of $[LZn_3]^{2+}$ and Mg^{2+}. Furthermore, no new signals (less than the detection limit of 3%) appeared in the ^{1}H NMR spectrum of $[LZn_3]^{3+}$ in the presence of Mg^{2+} (Figure 5a). The equilibrium constant K_{Mg} < 0.001 was

Scheme 6. Guest-Exchange Equilibrium

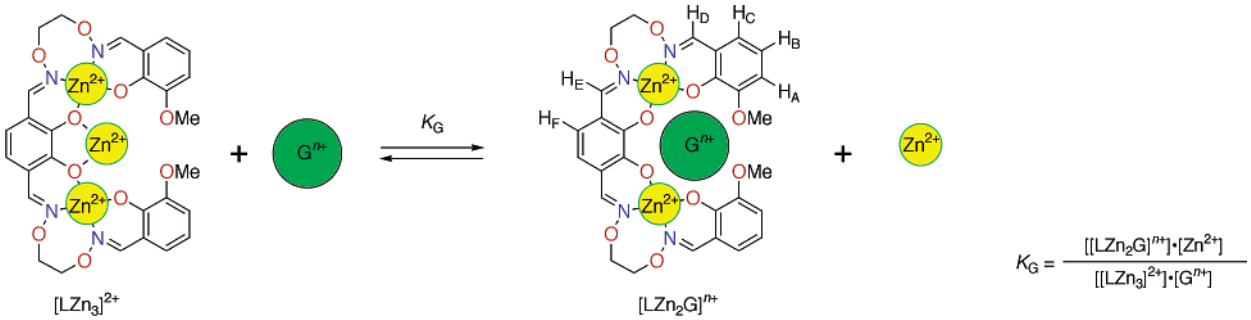

Table 1. Equilibrium Constants K_G for Metal Exchange

group 1		group 2		group 3	
Na^+	$<0.001^a$	Mg^{2+}	$<0.001^a$		
K^+	$<0.001^a$	Ca^{2+}	32 ± 3	Sc^{3+}	$>1000^b$
Rb^+	$<0.001^a$	Sr^{2+}	3.9 ± 0.6	Y^{3+}	$>1000^b$
Cs^+	$<0.001^a$	Ba^{2+}	0.16 ± 0.04	La^{3+}, Eu^{3+}, Lu^{3+}	$>1000^b$

[a] No new signal was detected (<3% intensity) when 1 equiv of G^{n+} was added. [b] $[LZn_3]^{2+}$ was completely (>97%) converted to $[LZn_2G]^{n+}$ when 1 equiv of G^{n+} was added.

calculated from the ^{1}H NMR data. From these values, Ca^{2+}/Mg^{2+} selectivity, which is biologically important, is estimated to be $\log(K_{Ca}/K_{Mg}) > 4.5$. A competition experiment confirmed the high Ca^{2+}/Mg^{2+} selectivity. Even when 10−1000 equiv of Mg^{2+} was added to an equimolar mixture of $[LZn_3]^{2+}$ and Ca^{2+} (1 mM), change of the concentration of $[LZn_2Ca]^{2+}$ was within ±6%. No new signals due to the Mg^{2+} complex were detected by ^{1}H NMR spectroscopy. These data indicate that the selectivity coefficient $\log(K_{Ca}/K_{Mg})$ is at least 5.1, which is similar to those of the excellent Ca^{2+} receptors or sensors such as BAPTA[23] (selectivity coefficients = 5.20), Quin2[23] (4.4), and K23E1[24] (5.0).

In contrast, UV−vis and ^{1}H NMR spectroscopies indicate that $[LZn_3]^{2+}$ has no affinity for alkali metal ions (Na^+, K^+, Rb^+, Cs^+) (Figure S4). Thus, among the biologically important metal cations (Na^+, K^+, Mg^{2+}, Ca^{2+}), the metallohost $[LZn_3]^{2+}$ exclusively recognizes Ca^{2+}.

The important point is that the metallohost $[LZn_3]^{2+}$ releases a Zn^{2+} ion when it binds a guest such as Ca^{2+}. In the neuronal function of the hippocampus, the amount of Zn^{2+} released is regulated by Ca^{2+} concentration.[25] From this point of view, the homotrinuclear complex $[LZn_3]^{2+}$ may work as a signal transducer by which molecular information is transferred into a different one.

Guest-Binding Selectivity of $[LZn_3]^{2+}$. Table 1 summarizes the guest-exchange equilibrium constants K_G for alkali, alkaline earth, and rare earth(III) metal ions. The metallohost $[LZn_3]^{2+}$ has very high selectivity to rare earth(III) ions ($K_G > 1000$) but did not show any interaction with alkali metal ions ($K_G < 0.001$). The equilibrium constants K_G for alkaline earth metals are in the range up to 32. Consequently, it can be concluded that the metallohost $[LZn_3]^{2+}$ is excellent in discriminating charge of the guest ions.

The equilibrium of the transmetalation shifts only when $[LZn_2G]^{n+}$ is more stable than $[LZn_3]^{2+}$. The selectivity probably comes from the electrostatic interaction between the two [Zn(salamo)] moieties and the guest cation G^{n+} in the resultant heterotrinuclear complex $[LZn_2G]^{n+}$. Because the phenolate oxygen atoms of the [Zn(salamo)] moieties are negatively charged, they can strongly interact with the positive charge of the guest ion. In the present case, a divalent zinc ion is initially bound to the central guest-binding site of the $[LZn_2]$. Alkali metal guests have no ability to replace the zinc ion probably because monovalent alkali metals interact with the $[LZn_2]$ moiety more weakly than the initially bound divalent zinc ion. On the other hand, trivalent rare earth ions interact strongly enough to replace the divalent zinc ion at the central O_6 site. The resultant metallohost−guest complexes $[LZn_2G]^{3+}$ (G = rare earth except for Tm^{3+}, Yb^{3+}, and Lu^{3+}) have four $ArO^-\cdots G^{3+}$ and two $Ar(Me)O^{\delta-}\cdots G^{3+}$ coordination bonds irrespective of the ionic radius of rare earth metals (vide infra). Accordingly, the metal exchange is mainly governed by charge−charge interaction arising from the six coordination bonds.

Among divalent alkaline earth metals having the same charge number as zinc(II), the size of the guest is also an important factor to determine the guest-binding strength. The experimental results demonstrated that the binding selectivity of the metallohost $[LZn_3]^{2+}$ is in the order of $Ca^{2+} > Sr^{2+} > Ba^{2+} \gg Mg^{2+}$. Obviously, Mg^{2+} is too small to interact effectively with all of the six oxygen donors of the O_6 site. On the other hand, Ca^{2+}, Sr^{2+}, and Ba^{2+}, whose equilibrium constants are between 0.16 and 32, can make six coordination bonds to an O_6 donor set (see X-ray structures). Among the three ions, Ca^{2+} has the highest equilibrium constant ($K_{Ca} = 32$). This result suggests that the O_6-binding site of the $[LZn_2]$ moiety has an appropriate size to bind Ca^{2+} with little distortion. The equilibrium constants for Sr^{2+} and Ba^{2+} are smaller than that for Ca^{2+}. This is probably because the complexation with larger alkaline earth metals (Sr^{2+} and Ba^{2+}) causes distortion of the $[LZn_2]$ moiety to destabilize the $[LZn_2G]^{2+}$.

From the viewpoint of controllable ion recognition, it is important to compare the binding affinity of $[LZn_3]^{2+}$ with that of H_4L. ^{1}H NMR spectroscopic study clearly showed that the free ligand H_4L did not interact with alkali, alkaline earth, and lanthanide ions. The results also support the importance of rigid conformation having an O_6 site as well as charge−charge interaction between the $[LZn_2]$ moiety and guest ions. When zinc(II) ions are absent, the flexible conformation of H_4L may reduce the affinity of the six oxygen donors to cationic guests. The weaker affinity is also due to the absence of negative charge in the ligand H_4L in phenol form. There is only dipole−charge interaction, much weaker than charge−charge interaction, between guest ions and the host.

Crystal Structures of Heterotrinuclear Complexes. The guest G^{n+} of the heterotrinuclear complexes $[LZn_2G]^{n+}$ is accommodated in the central O_6 site. If all six oxygen donors of the central O_6 site coordinate to the guest ion, the ligand moiety forms a helix in such a way that the two terminal methoxy groups are close to one another. X-ray crystallographic analysis revealed the molecular structures of the heterotrinuclear complexes $[LZn_2G]^{n+}$ (Figures 6 and S5−S7).

In all cases, two zinc atoms are 5- or 6-coordinate and sit in the N_2O_2 salamo chelate moieties. The guest metal G^{n+} is in the central O_6 site. When rare earth metals are used as G^{n+}, the coordination number of the G^{n+} depends on the ionic radius (10-coordinate for La^{3+}, 9-coordinate for Y^{3+}, and 8-coordinate for Sc^{3+}) (Scheme 7). The corresponding Ce^{3+}−Er^{3+} complexes are similar to the Y^{3+} complex with a 9-coordinate metal center, but there are slight differences in the coordination mode of anions and solvent molecules. As expected, the ligand moiety adopts a helical conformation surrounding the guest metal G^{n+}. All of the oxygen donors of the O_6 site including methoxy groups effectively coordinate to the central guest metal G^{n+}.[26] In addition, anions and solvent molecules coordinate to the Zn−G−Zn core. Smaller lanthanides, Tm^{3+}, Yb^{3+}, and Lu^{3+}, gave an "open-type" complex, where two of the O_6 donors do not form coordination bonds with G^{n+} (Scheme 7). In contrast, all

(22) Switzer, M. E. *Sci. Prog.* **1978**, *65*, 19−30.
(23) Tsien, R. Y. *Biochemistry* **1980**, *19*, 2396−2404.
(24) Suzuki, K.; Watanabe, K.; Matsumoto, Y.; Kobayashi, M.; Sato, S.; Siswanta, D.; Hisamoto, H. *Anal. Chem.* **1995**, *67*, 324−334.
(25) Assaf, S. Y.; Chung, S.-H. *Nature* **1984**, *308*, 734−736.

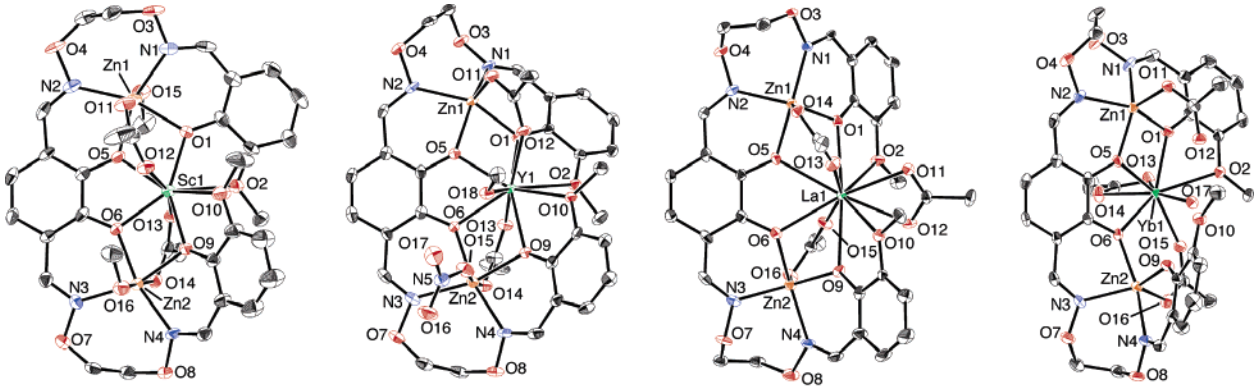

Figure 6. X-ray structures of $[LZn_2Sc]^{3+}$, $[LZn_2Y]^{3+}$, $[LZn_2La]^{3+}$, and $[LZn_2Yb]^{3+}$.

Scheme 7. Schematic Representation of the Crystal Structures of Helical Trinuclear Complexes $[LZn_2G]^{n+}$

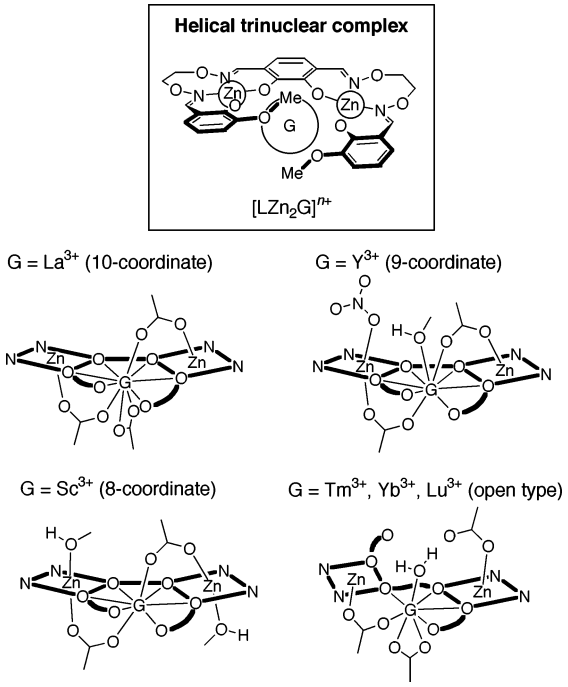

three alkaline earth metal (Ca^{2+}, Sr^{2+}, and Ba^{2+}) formed helical complexes with an 8-coordinate G^{n+} irrespective of the ionic radius. Further information about the crystal structures is included in the Supporting Information (Scheme S1 and Figures S5−S7).

The geometrical parameters of the helical heterotrinuclear metallohost−guest complexes $[LZn_2G]^{n+}$ are summarized in Table 2. The radius d and winding angles θ of the helix are defined as averaged G−O distances and the sum of five O−G−O angles, respectively. Among rare earth metals, larger lanthanides (La, Ce, Pr, etc.) have longer d and smaller winding angle θ (Figure 7). Consequently, the ligand wraps the most loosely around La^{3+}. On the contrary, a complex of the smallest rare earth, Sc^{3+}, has the largest winding angle ($\theta = 345°$). In the case of alkaline earth metals, the two parameters d and θ similarly depend on the sizes of Ca^{2+}, Sr^{2+}, and Ba^{2+}.

Table 2. Geometrical Features of Heterotrinuclear Complexes $[LZn_2G]^{n+}$ Determined by X-ray Crystallography

G	N_M[a]	d/Å[b]	θ/deg[c]
La^{3+}	10	2.695	288.5
Ce^{3+}	9	2.532	320.5
Pr^{3+}	9	2.518	321.6
Nd^{3+}	9	2.496	322.8
Sm^{3+}	9	2.481	324.6
Eu^{3+}	9	2.472	325.5
Gd^{3+}	9	2.461	326.3
Tb^{3+}	9	2.443	323.9
Dy^{3+}	9	2.444	324.5
Ho^{3+}	9	2.435	325.3
Er^{3+}	9	2.430	326.0
Tm^{3+}	8	2.376[d]	
Yb^{3+}	8	2.370[d]	
Lu^{3+}	8	2.359[d]	
Sc^{3+}	8	2.271, 2.260[e]	344.6, 345.1[e]
Y^{3+}	9	2.412	326.1
Ca^{2+}	8	2.469	316.6
Sr^{2+}	8	2.576	308.8
Ba^{2+}	8	2.719	296.4

[a] Number of donor atoms coordinating to guest metal G. [b] Average of the distances G−O1, G−O2, G−O5, G−O6, G−O9, and G−O10. [c] Winding angle of the single helix defined as the sum of the angles of O2−G−O1, O1−G−O5, O5−G−O6, O6−G−O9, and O9−G−O10. [d] Average of the distances G−O1, G−O2, G−O5, and G−O6. [e] Two independent molecules in the unit cell.

Thus, the metallohost−guest complexes are "metallohelicenes", in which ligand L^{4-} and zinc(II) constitute a helically arranged π-conjugate system.[27] Guest ion G^{n+} fits inside the helical structure. The winding angle can be set at various values by choosing the guest cation G^{n+}. Accordingly, the helical complexes are regarded as a "tunable" molecular spring or coil, whose radius and winding angles can be modulated by changing the central guest ion (Figure 8).

Conformation of Heterotrinuclear Complexes in Solution. The conformation of the heterotrinuclear complexes $[LZn_2G]^{n+}$ in solution was investigated by ^1H NMR spectroscopy (Table 3). Although chemical shifts of the aromatic and oxime protons (H_A−H_F) did not change significantly (within 0.3 ppm) by changing the guest metal G^{n+}, resonance of the methoxy groups strongly depended on G^{n+}. The methoxy proton of $[LZn_2Sc]^{3+}$ was observed at 3.45 ppm, higher field than that of $[LZn_3]^{2+}$.

(26) Coordination of methoxy groups to lanthanide metal is found in $[(3\text{-MeOsalamo})_2Zn_2La]^{3+}$ and $[(3\text{-MeOsalamo})ZnLu]^{3+}$, see: Akine, S.; Taniguchi, T.; Nabeshima, T. *Chem. Lett.* **2006**, *35*, 604−605.

(27) (a) Dai, Y.; Katz, T. J.; Nichols, D. A. *Angew. Chem., Int. Ed. Engl.* **1996**, *35*, 2109−2111. (b) Dai, Y.; Katz, T. J. *J. Org. Chem.* **1997**, *62*, 1274−1285. (c) Zhang, H.-C.; Huang, W.-S.; Pu, L. *J. Org. Chem.* **2001**, *66*, 481−487. (d) Zhang, F.; Bai, S.; Yap, G. P. A.; Tarwade, V.; Fox, J. M. *J. Am. Chem. Soc.* **2005**, *127*, 10590−10599.

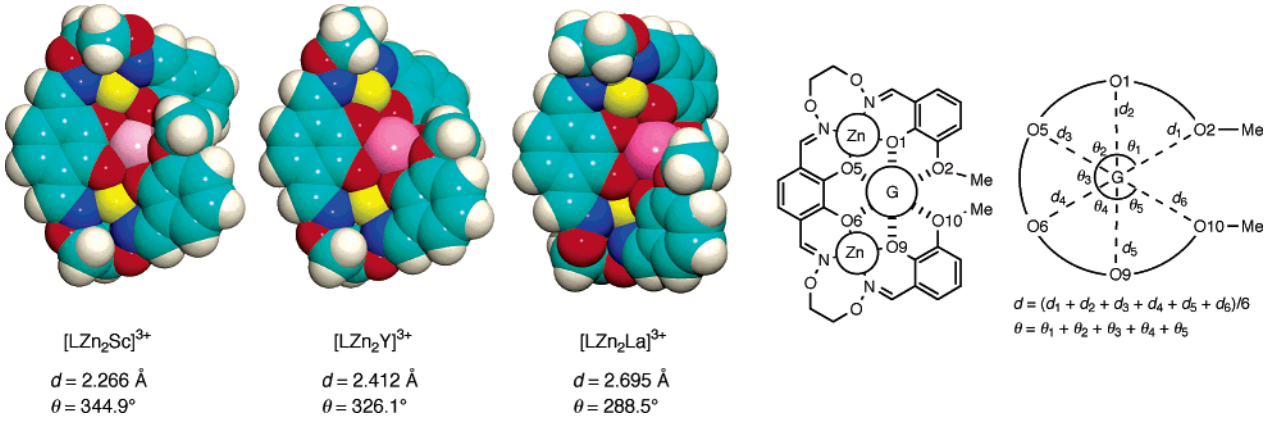

Figure 7. Space-filling representation of the crystal structure of $[LZn_2G]^{3+}$ (G = Sc^{3+}, Y^{3+}, La^{3+}), showing their helical conformation. Counter anions and solvent molecules coordinating to metals are not shown.

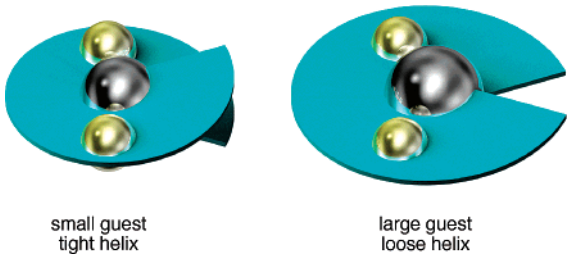

Figure 8. Schematic drawing of tunable helical complexes $[LZn_2G]^{n+}$.

This can be attributed to the tightly winded helical conformation of $[LZn_2Sc]^{3+}$. The large upfield shift of the methoxy proton can be reasonably explained in terms of shielding by the other terminal aromatic ring of the ligand. On the other hand, the methoxy protons appeared at lower field when G^{n+} has a larger ionic radius. In the case of $[LZn_2La]^{3+}$, the proton was observed at 4.08 ppm, lower than $[LZn_2Sc]^{3+}$ by 0.63 ppm. This suggests that $[LZn_2La]^{3+}$ forms a loose helix in which the two terminals of the ligand are apart from each other.

It is noteworthy that $[LZn_2Lu]^{3+}$ also showed a symmetric ^{1}H NMR pattern although the complex has an unsymmetrical "open-type" conformation in the crystalline state. Probably, the complex has a helical conformation in solution.

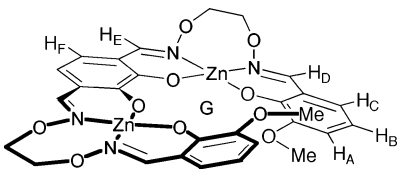

Conclusion

We have designed a new type of bis(N_2O_2) chelate ligand that affords a C-shaped O_6 site on the metalation of the N_2O_2 sites. UV−vis and ^{1}H NMR titration clearly showed that the complexation between H_4L and zinc(II) acetate affords 1:3 complex $[LZn_3]^{2+}$ via a highly cooperative process. Although the O_6-recognition site of the dinuclear metallohost $[LZn_2]$ is filled with the additional Zn^{2+}, the O_6 site can bind a guest ion with concomitant release of the initially bound Zn^{2+}. In the novel recognition process "guest exchange" utilizing the homotrinuclear zinc(II) complex $[LZn_3]^{2+}$, interesting guest selectivity was observed. The exchange took place quantitatively when rare earth metals were used as a guest. In the case of alkaline earth metals, selectivity of $Ca^{2+} > Sr^{2+} > Ba^{2+} \gg Mg^{2+}$ was observed. On the other hand, the transmetalation did not take place at all when alkali metals were used for the guest. Accordingly, the metallohost $[LZn_3]^{2+}$ is excellent in discriminating charge of the guest ions. The observed Ca^{2+} selectivity among the alkaline earth metals can be explained by the size-fit principle. In this recognition system, the guest ion selectively replaces the metal in the central O_6 site, probably due to the effective coordination of six oxygen donors of the helical O_6 site to the guest metal G^{n+}. The metallohost−guest complexes thus obtained are a kind of "metallohelicene" because they have a helically arranged π-conjugate system. The geometrical parameters of helix, radius d and winding angle θ, depend on the size of the guest. The La^{3+} complex has the smallest θ (288°), and the Sc^{3+} complex has the largest θ (345°). Because the radius and winding angles of helices are tunable by changing the guest ion, the helical metallohost−guest complexes are regarded as a molecular spring or coil. Consequently, site-specific metal exchange of trinuclear complex $[LZn_3]^{2+}$ described here will be utilized for highly selective ion recognition, site-selective synthesis of $(3d)_2(4f)$ trimetallic complexes, and construction of "tunable" metallohelicenes. Different nature of the N_2O_2 and O_6 sites of the well-programmed ligand H_4L is crucial for the multifunctionality.

Table 3. Chemical Shift of Selected Protons of Diamagnetic Heterotrinuclear Complexes $[LZn_2G]^{n+}$ in $CDCl_3/CD_3OD$ (1:1)

	OMe	H_A	H_B	H_C	H_D	H_E	H_F	d(O–G)[a]
LZn_3	3.79	6.90	6.65	6.80	8.32	8.65	6.63	
LZn_2Ca	3.74	6.99	6.69	6.91	8.51	8.47	6.50	2.469
LZn_2Sc	3.45	6.92	6.83	6.99	8.38	8.31	6.64	2.266[b]
LZn_2Y	3.93	7.13	6.79	7.01	8.60	8.44	6.63	2.412
LZn_2La	4.08	7.16	6.78	7.01	8.62	8.45	6.65	2.695
LZn_2Lu	3.75	7.06	6.81	7.01	8.48	8.39	6.62	2.359

[a] Average O−G distances determined by X-ray crystallography. [b] Average of the two crystallographically independent molecules.

The characteristic helical frameworks of the heteronuclear metal complexes obtained here would be applied to chiral recognition, when a chiral auxiliary is introduced into the ligands. In addition, the multi-metal cores may provide an effective multibinding site for anions and a catalytic site for various organic reactions as well. If the metals in the complexes are paramagnetic, novel magnetic properties are expected due to 3d−3d and 3d−4f magnetic exchange. These kinds of synergetic functions at the molecular level are our next challenging target to achieve more sophisticated intelligent molecules by using the multisalamo metal complexes.

Experimental Section

General. All experiments were carried out in air unless otherwise noted. Diethyl ether was distilled from sodium benzophenone ketyl prior to use. *N*,*N*,*N*′,*N*′-Tetramethylethylenediamine, *N*,*N*-dimethylformamide, and dichloromethane were distilled from calcium hydride prior to use. Commercial chloroform and ethanol were used without further purification. All chemicals were of reagent grade and used as received. ^{1}H and ^{13}C NMR spectra were recorded on a Bruker AC300 (300 and 75 MHz) or ARX400 (400 and 100 MHz) spectrometer. Mass spectra (ESI-TOF, positive mode) were recorded on an Applied Biosystems QStar Pulsar *i* spectrometer.

Caution: *Metal perchlorates are potentially explosive. Only a small amount of material should be prepared, and it should be handled with great care.*

Synthesis of 2,3-Dimethoxybenzene-1,4-dicarbaldehyde (1). To a solution of *o*-dimethoxybenzene (2.76 g, 20 mmol) and *N*,*N*,*N*′,*N*′-tetramethylethylenediamine (15 mL, 100 mmol) in diethyl ether (70 mL) was added *n*-butyllithium (2.6 M solution in hexane, 39 mL, 100 mmol) at 0 °C under argon atmosphere. The mixture was heated to reflux for 20 h. After the mixture was cooled to room temperature, *N*,*N*-dimethylformamide (8.6 mL, 110 mmol) was added to the mixture, which was stirred overnight at room temperature. After addition of water (50 mL), the mixture was extracted with chloroform. The organic layer was dried over anhydrous magnesium sulfate, filtered, and concentrated to give a reddish brown oil. The residue was then chromatographed on silica gel (chloroform) to give a pale yellow solid, which was further purified by recrystallization from dichloromethane/hexane to afford 2,3-dimethoxybenzene-1,4-dicarbaldehyde (**1**) (1.55 g, 40%) as pale yellow crystals, mp 100−101 °C. ^{1}H NMR (400 MHz, $CDCl_3$): δ 4.06 (s, 6H), 7.64 (s, 2H), 10.45 (s, 2H). ^{13}C NMR (100 MHz, $CDCl_3$): δ 62.41 (CH_3), 122.76 (CH), 134.17 (C), 156.61 (C), 189.16 (CHO). Anal. Calcd for $C_{10}H_{10}O_4$: C, 61.85; H, 5.19. Found: C, 61.89; H, 5.53.

Synthesis of 2,3-Dihydroxybenzene-1,4-dicarbaldehyde (2). To a solution of 2,3-dimethoxybenzene-1,4-dicarbaldehyde (**1**) (1.59 g, 8.19 mmol) in dichloromethane (70 mL) was added boron tribromide (3.1 mL, 32.8 mmol) under nitrogen atmosphere. After the mixture was stirred for 4 h at room temperature, water (70 mL) was added to the mixture, which was further stirred overnight. The mixture was extracted with chloroform, and the organic layer was dried over anhydrous magnesium sulfate, filtered, and concentrated to dryness. The residue was recrystallized from chloroform/hexane to give dialdehyde **2** (1.29 g, 95%) as yellow crystals, mp 140−143 °C. ^{1}H NMR (300 MHz, $CDCl_3$): δ 7.28 (s, 2H), 10.03 (s, 2H), 10.91 (s, 2H). ^{13}C NMR (100 MHz, $CDCl_3$): δ 122.15 (CH), 123.24 (C), 150.77 (C), 196.18 (CHO). Anal. Calcd for $C_8H_6O_4$: C, 57.84; H, 3.64. Found: C, 57.35; H, 3.74.

Synthesis of Ligand H_4L. To a solution of monooxime **3a** (R = OMe)[11c] (271.7 mg, 1.20 mmol) in ethanol (20 mL) was gradually added a solution of 2,3-dihydroxybenzene-1,4-dicarbaldehyde (**2**) (99.7 mg, 0.60 mmol) in ethanol (20 mL). The mixture was heated for 40 min at 50−55 °C and cooled to room temperature. The white precipitates were collected to give H_4L (307.1 mg, 88%) as colorless crystals, mp 147−148 °C. ^{1}H NMR (300 MHz, $CDCl_3$): δ 3.91 (s, 6H), 4.49−4.52 (m, 8H), 6.77 (s, 2H), 6.83−6.91 (m, 6H), 8.23 (s, 2H), 8.26 (s, 2H), 9.64 (s, 2H), 9.73 (s, 2H). ^{13}C NMR (75 MHz, $CDCl_3$): δ 56.19 (CH_3), 73.02 (CH_2), 73.18 (CH_2), 113.72 (CH), 116.51 (C), 117.62 (C), 119.42 (CH), 120.63 (CH), 122.36 (CH), 145.69 (C), 147.14 (C), 148.15 (C), 151.13 (CH), 151.82 (CH). Anal. Calcd for $C_{28}H_{30}N_4O_{10}$: C, 57.73; H, 5.19; N, 9.62. Found: C, 57.41; H, 5.45; N, 9.49.

Synthesis of Ligand H_4L′. To a solution of monooxime **3b** (R = H)[11c] (275.0 mg, 1.40 mmol) in ethanol (20 mL) was gradually added a solution of 2,3-dihydroxybenzene-1,4-dicarbaldehyde (**2**) (116.3 mg, 0.70 mmol) in ethanol (20 mL). The mixture was heated for 1 h at 50−55 °C and cooled to room temperature. The white precipitates were collected to give H_4L′ (243 mg, 66%) as colorless crystals, mp 142−143 °C. ^{1}H NMR (400 MHz, $CDCl_3$): δ 4.48−4.52 (m, 8H), 6.77 (s, 2H), 6.90 (t, J = 7.6 Hz, 2H), 6.97 (d, J = 7.6 Hz, 2H), 7.16 (d, J = 7.6 Hz, 2H), 7.28 (t, J = 7.6 Hz, 2H), 8.23 (s, 2H), 8.25 (s, 2H), 9.65 (s, 2H), 9.73 (s, 2H). ^{13}C NMR (75 MHz, $CDCl_3$): δ 72.96 (CH_2), 73.32 (CH_2), 116.16 (C), 116.76 (CH), 117.61 (C), 119.65 (CH), 120.80 (CH), 130.93 (CH), 131.39 (CH), 145.79 (C), 151.37 (CH), 152.35 (CH), 157.42 (C). Anal. Calcd for $C_{26}H_{26}N_4O_8$: C, 59.77; H, 5.02; N, 10.72. Found: C, 59.45; H, 5.02; N, 10.80.

Synthesis of Zinc(II) Complex [$LZn_3(OAc)_2$]. A solution of zinc(II) acetate dihydrate (26.3 mg, 0.12 mmol) in ethanol (10 mL) was added to a solution of ligand H_4L (23.3 mg, 0.040 mmol) in chloroform/ethanol (1:4, 10 mL). After the resulting solution was allowed to stand at room temperature, the precipitates were collected to afford the complex (30.9 mg, 82%) as yellow crystals. ^{1}H NMR (400 MHz, $CDCl_3$): δ 2.09 (s, 6H), 3.61 (s, 6H), 3.93 (dd, J = 13.9, 1.8 Hz, 2H), 4.11 (dd, J = 15.2, 4.2 Hz), 4.32 (t, J = 12.1 Hz, 2H), 5.43 (t, J = 13.0 Hz, 2H), 6.44 (s, 2H), 6.48 (t, J = 7.8 Hz, 2H), 6.67 (dd, J = 7.8, 1.5 Hz, 2H), 6.75 (dd, J = 7.8, 1.5 Hz, 2H), 8.20 (s, 2H), 8.35 (s, 2H). Anal. Calcd for $C_{32}H_{32}N_4O_{14}Zn_3\cdot 3H_2O$: C, 40.59; H, 4.05; N, 5.92. Found: C, 40.66; H, 3.95; N, 5.86.

Synthesis of Zinc(II) Complex [L′$Zn_3(OAc)_2$]. A solution of zinc(II) acetate dihydrate (9.9 mg, 0.045 mmol) in ethanol (5 mL) was added to a solution of ligand H_4L′ (7.8 mg, 0.015 mmol) in chloroform/ethanol (1:4, 5 mL). The resulting solution was concentrated to dryness, and the residue was recrystallized from acetone/hexane to afford the complex (7.3 mg, 52%) as yellow crystals. ^{1}H NMR (400 MHz, $CDCl_3$): δ 2.15 (s, 6H), 4.21 (dd, J = 12.5, 2.4 Hz, 2H), 4.22 (dd, J = 15.2, 4.5 Hz, 2H), 4.46 (td, J = 12.5, 4.5 Hz, 2H), 5.57 (ddd, J = 15.2, 12.5, 2.4 Hz, 2H), 6.51 (s, 2H), 6.62 (t, J = 7.4 Hz, 2H), 6.83 (d, J = 8.4 Hz, 2H), 7.04 (dd, J = 7.4, 1.7 Hz, 2H), 7.20 (ddd, J = 8.4, 7.4, 1.7 Hz, 2H), 8.19 (s, 2H), 8.52 (s, 2H). Anal. Calcd for $C_{30}H_{28}N_4O_{12}Zn_3\cdot 3H_2O\cdot Me_2CO$: C, 41.95; H, 4.27; N, 5.93. Found: C, 42.18; H, 3.81; N, 5.82.

Preparation of [$LZn_2Ln(OAc)_3$]. A solution of zinc(II) acetate dihydrate (4.4 mg, 0.020 mmol) in methanol (1 mL) and a solution of $Ln(OAc)_3\cdot nH_2O$ (Ln = lanthanide; 0.010 mmol) in water/methanol (1:4, 1 mL) were added to a solution of H_4L (5.8 mg, 0.010 mmol) in chloroform (1 mL), and the resulting solution was concentrated to dryness. Vapor-phase diffusion of diethyl ether into a chloroform/methanol solution of the residue gave yellow crystals of [$LZn_2Ln(OAc)_3$].

[$LZn_2La(OAc)_3$]. Yield 77%. Anal. Calcd for $C_{34}H_{35}LaN_4O_{16}Zn_2\cdot CHCl_3$: C, 36.72; H, 3.17; N, 4.89. Found: C, 37.13; H, 3.41; N, 4.87.

[$LZn_2Ce(OAc)_3$]. Yield 78%. Anal. Calcd for $C_{34}H_{35}CeN_4O_{16}Zn_2\cdot 3MeOH\cdot 0.75CHCl_3$: C, 37.40; H, 3.97; N, 4.62. Found: C, 37.43; H, 3.82; N, 4.53.

[$LZn_2Pr(OAc)_3$]. Yield 73%. Anal. Calcd for $C_{34}H_{35}N_4O_{16}PrZn_2\cdot 3MeOH\cdot CHCl_3$: C, 36.72; H, 3.89; N, 4.51. Found: C, 37.03; H, 3.72; N, 4.53.

[$LZn_2Nd(OAc)_3$]. Yield 92%. Anal. Calcd for $C_{34}H_{35}N_4NdO_{16}Zn_2\cdot 3MeOH\cdot CHCl_3$: C, 36.62; H, 3.88; N, 4.50. Found: C, 36.64; H, 3.61; N, 4.53.

[$LZn_2Sm(OAc)_3$]. Yield 82%. Anal. Calcd for $C_{34}H_{35}N_4O_{16}SmZn_2 \cdot 3MeOH \cdot 0.5CHCl_3$: C, 37.77; H, 4.01; N, 4.70. Found: C, 37.72; H, 3.86; N, 5.04.

[$LZn_2Eu(OAc)_3$]. Yield 85%. Anal. Calcd for $C_{34}H_{35}EuN_4O_{16}Zn_2 \cdot 3MeOH \cdot 0.5CHCl_3$: C, 37.72; H, 4.01; N, 4.69. Found: C, 37.42; H, 3.85; N, 4.45.

[$LZn_2Gd(OAc)_3$]. Yield 91%. Anal. Calcd for $C_{34}H_{35}GdN_4O_{16}Zn_2 \cdot H_2O$: C, 38.46; H, 3.51; N, 5.28. Found: C, 38.10; H, 3.65; N, 5.00.

[$LZn_2Tb(OAc)_3$]. Yield 83%. Anal. Calcd for $C_{34}H_{35}N_4O_{16}TbZn_2 \cdot H_2O \cdot MeOH$: C, 38.38; H, 3.77; N, 5.11. Found: C, 38.72; H, 3.81; N, 4.76.

[$LZn_2Dy(OAc)_3$]. Yield 68%. Anal. Calcd for $C_{34}H_{35}DyN_4O_{16}Zn_2 \cdot 2H_2O$: C, 37.64; H, 3.62; N, 5.16. Found: C, 37.54; H, 3.87; N, 5.12.

[$LZn_2Ho(OAc)_3$]. Yield 78%. Anal. Calcd for $C_{34}H_{35}HoN_4O_{16}Zn_2 \cdot MeOH \cdot H_2O \cdot Et_2O$: C, 39.85; H, 4.37; N, 4.77. Found: C, 39.43; H, 4.11; N, 4.55.

[$LZn_2Er(OAc)_3$]. Yield 70%. Anal. Calcd for $C_{34}H_{35}ErN_4O_{16}Zn_2 \cdot 2H_2O \cdot Et_2O$: C, 39.22; H, 4.24; N, 4.81. Found: C, 38.98; H, 4.25; N, 4.73.

[$LZn_2Tm(OAc)_3$]. Yield 83%. Anal. Calcd for $C_{34}H_{35}N_4O_{16}TmZn_2 \cdot H_2O \cdot 0.5CHCl_3$: C, 36.57; H, 3.34; N, 4.94. Found: C, 36.52; H, 3.41; N, 4.63.

[$LZn_2Yb(OAc)_3$]. Yield 79%. Anal. Calcd for $C_{34}H_{35}N_4O_{16}YbZn_2 \cdot H_2O \cdot 0.75CHCl_3$: C, 35.76; H, 3.26; N, 4.80. Found: C, 35.80; H, 3.22; N, 4.58.

[$LZn_2Lu(OAc)_3$]. Yield 83%. Anal. Calcd for $C_{34}H_{35}LuN_4O_{16}Zn_2 \cdot H_2O \cdot 0.5CHCl_3$: C, 36.38; H, 3.32; N, 4.92. Found: C, 36.44; H, 3.41; N, 4.66.

Preparation of [$LZn_2G(OAc)_2(NO_3)$] (G = Sc, Y). Solutions of zinc(II) acetate dihydrate (6.6 mg, 0.030 mmol) in ethanol (4 mL) and $G(NO_3)_3 \cdot nH_2O$ (G = Sc, Y; 0.010 mmol) in ethanol (4 mL) were added to a solution of H_4L (5.8 mg, 0.010 mmol) in chloroform/ethanol (1:2, 3 mL), and the resulting solution was concentrated to dryness. Vapor-phase diffusion of diethyl ether into chloroform/methanol solution of the residue gave yellow crystals of $LZn_2G(OAc)_2(NO_3)$.

[$LZn_2Sc(OAc)_2](NO_3)$. Yellow crystals, yield 75%. Anal. Calcd for $C_{32}H_{32}N_5O_{17}ScZn_2 \cdot 2MeOH \cdot H_2O$: C, 40.18; H, 4.16; N, 6.89. Found: C, 39.94; H, 4.36; N, 6.55.

[$LZn_2Y(OAc)_2(NO_3)$]. Yellow crystals, yield 73%. Anal. Calcd for $C_{32}H_{32}N_5O_{17}YZn_2 \cdot 3H_2O$: C, 37.23; H, 3.71; N, 6.78. Found: C, 37.17; H, 3.85; N, 6.84.

Preparation of [$LZn_2G(OAc)_2$] (G = Ca, Sr, Ba). Solutions of zinc(II) acetate dihydrate (4.4 mg, 0.020 mmol) in methanol (1 mL) and $G(OAc)_2$ (G = Ca, Sr, Ba; 0.010 mmol) in water/methanol (1:3, 2 mL) were added to a solution of H_4L (5.8 mg, 0.010 mmol) in chloroform (1 mL), and the resulting solution was concentrated to dryness. Vapor-phase diffusion of diethyl ether into the chloroform/methanol solution of the residue gave yellow crystals of [$LZn_2G(OAc)_2$].

[$LZn_2Ca(OAc)_2$]. Yellow crystals, yield 77%. Anal. Calcd for $C_{32}H_{32}CaN_4O_{14}Zn_2 \cdot 0.75CHCl_3$: C, 41.10; H, 3.45; N, 5.85. Found: C, 40.88; H, 3.39; N, 5.69.

[$LZn_2Sr(OAc)_2$]. Yellow crystals, yield 77%. Anal. Calcd for $C_{32}H_{32}N_4O_{14}SrZn_2 \cdot 0.75CHCl_3$: C, 39.16; H, 3.29; N, 5.58. Found: C, 39.26; H, 3.28; N, 5.42.

[$LZn_2Ba(OAc)_2$]. Yellow crystals, yield 84%. Anal. Calcd for $C_{32}H_{32}BaN_4O_{14}Zn_2$: C, 39.84; H, 3.34; N, 5.81. Found: C, 40.09; H, 3.61; N, 5.45.

X-ray Crystallographic Analysis of Heterotrinuclear Complexes. Intensity data were collected on a Rigaku RAXIS Rapid or a Rigaku Mercury CCD diffractometer with Mo Kα radiation ($\lambda = 0.71069$ Å). Reflection data were corrected for Lorentz and polarization factors and for absorption using the multiscan method. The structure was solved by Patterson methods (DIRDIF 99)[28] or direct methods (SIR 97[29] or SHELXS 97[30]) and refined by full-matrix least-squares on F^2 using SHELXL 97.[31] The crystallographic data are summarized in Table S1.

Acknowledgment. We thank Mr. Takashi Matsumoto for technical assistance with the preparation of [$LZn_2G(OAc)_2$] (G = alkaline earth). This work was supported by Grants-in-Aid for Scientific Research from the Ministry of Education, Culture, Sports, Science, and Technology, Japan.

Supporting Information Available: Spectroscopic titration and X-ray crystallographic data (CIF). This material is available free of charge via the Internet at http://pubs.acs.org.

JA0646702

(28) Beurskens, P. T.; Beurskens, G.; de Gelder, R.; Garcia-Granda, S.; Gould, R. O.; Israel R.; Smits, J. M. M. *The DIRDIF-99 program system*; Crystallography Laboratory, University of Nijmegen, The Netherlands, 1999.
(29) SIR 97, program for crystal structure solution. Altomare, A.; Burla, M. C.; Camalli, M.; Cascarano, G. L.; Giacovazzo, C.; Guagliardi, A.; Moliterni, A. G. G.; Polidori, G.; Spagna, R. *J. Appl. Crystallogr.* **1999**, *32*, 115−119.
(30) Sheldrick, G. M. *SHELXS 97, Program for crystal structure determination*; University of Göttingen, Germany, 1997.
(31) Sheldrick, G. M. *SHELXL 97, Program for crystal structure determination*; University of Göttingen, Germany, 1997.